

Chapter 3

Model Systems

In the previous section, the various features of condensed phase dynamics were discussed. Theoretical simulation can help to resolve the experimental observations of these processes and phenomena. Matrix isolated iodine was investigated very thoroughly. Some of the aforementioned effects could be found in this system, like in studies concerning the construction of the potential surfaces [65], the cage effect and with it dissociation and recombination [61, 62, 63], to mention only some of them. Then topics like vibrational relaxation, including pumping to the forbidden B-state with its triplet character were investigated [64]. Shock waves were calculated by Martens [43] and the dynamics including phonon excitation has been reviewed by Apkarian [60] and Schwentner [41]. Additionally there is to mention the Ph.D Thesis of Matias Bargheer [40], who investigated I_2 , Cl_2 and ClF in solid rare gases.

One great advantage of the system iodine in krypton or argon is the availability of experimental results, as has been shown in 1.5.2. Recently, an increasing number of experiments have been performed for different dihalogens in rare gas matrices, like Br_2 in Ar, ClF in Ar and Cl_2 in Ar. The investigation of these systems, by theory and experiment, respectively, can probably give more insight into topics, which were not apparent in the case of iodine. Iodine is a heavy atom and thus behaves more like a classical particle. The systems mentioned before, especially Cl_2 and ClF , consist of lighter atoms, and especially in the latter case quantum effects could be expected, due to the light fluorine atom. Each of these dihalogens has its own characteristics and thus their investigation would reveal information on these particular features. Therefore, the choice of the system will depend on the focus of the investigation and on the characteristic properties of the system itself. For

the analysis of predissociation, bromine and iodine would be favourable, since chlorine or chlorinefluoride show no avoided crossings of the adiabatic potentials at internuclear distances close to equilibrium, where the influence of the matrix is not playing the dominant role. On the other hand, ClF and Cl₂ will be preferable if this effect should be neglected and for more detailed information about quantum effects. The aim of this work was to constitute an appropriate model system, which may have some similar properties as iodine in rare gas systems, but on the other hand would reveal a more complex dynamics, including effects of quantum nature like transitions between the adiabatic states.

A system which has been investigated in the gas phase very thoroughly and where experimental results in rare gas environment are also available, is Cl₂. Photodissociation of matrix isolated molecular chlorine was investigated by several groups, for example [68, 69, 70, 72]. Simulations focussing on the guest-host dynamics have been performed by Ovchinikov and Apkarian [34] and experimental results for the electronic relaxation after photoexcitation for crystalline chlorine was compared to the system Cl₂ in Ar, emphasizing the role of the environment [71].

Fig. 3.1 shows the gas phase potentials of Cl₂ of the four lowest valence states without spin orbit coupling, calculated by Kokh et al [47].

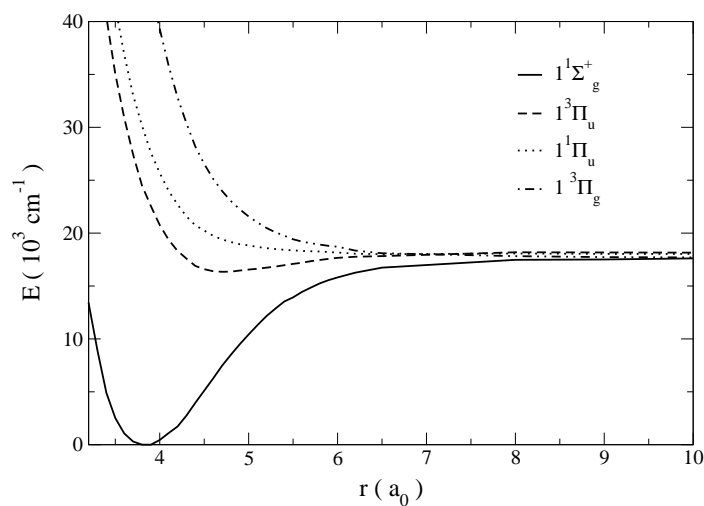


Figure 3.1: *Calculated potential energy curves of Cl₂ of the four lowest lying valence states without spin-orbit coupling, data provided by Daria Kokh [47]*

Comparing to the potentials of iodine in krypton calculated by Batista [73], see Fig. 1.15, at internuclear distances, where the environment is not expected to play a crucial role (e.g. in the case of iodine for distances smaller than approx. 4 Å), there are no crossings of the states. Even though the spin-orbit coupling would lift the degeneracy of the states, the splitting is comparatively small and would not significantly change the shape of the potentials. By this it can be assumed that even after the modification of the potentials due to the influence of the environment, no predissociation will occur. The $^1\Pi_u$ state is the lowest state, to which excitation is optically allowed, and the energetically lower $^3\Pi_u$ state is well separable up to an internuclear distance of $5.5 a_0$. Thus, Cl_2 should be a system useful for investigation of recombination and vibrational relaxation without any influence by predissociation.

The next step is to introduce the halogen in a rare gas matrix. Argon is preferable for several reasons. First, the equilibrium geometry of molecular chlorine embedded in an argon matrix is supposed to be similar to the system iodine in krypton, facilitating comparison to the latter system. Due to the similar van-der-Waals radii of the halogen and rare gas atoms, the guest molecules occupy a double substitutional site of the lattice, compare Fig. 3.2 and Fig. 1.3.

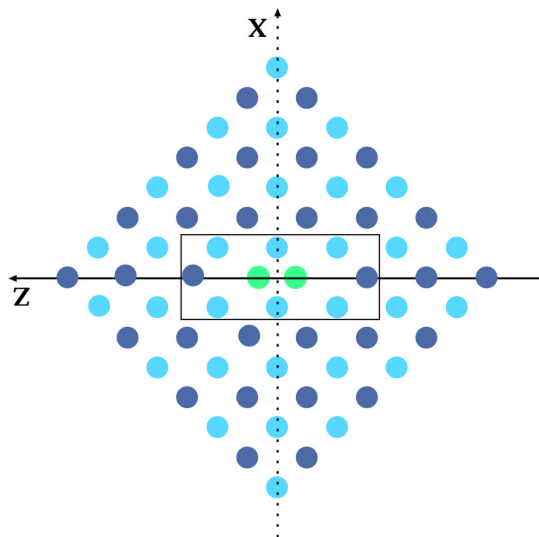


Figure 3.2: Orientation of X_2 in Ar, $X = \text{Cl}, \text{I}$. Dark shading depict atoms in the layer containing the halogen molecule, light shading atoms in the layers above or below.

Taking into account the diameter of the disubstitutional sites (3.71 Å for Ar, 4.03 Å for Kr) and the space occupied by the impurity molecules (bond length plus van-der-Waals radii), there is more space available for the chlorine in the argon matrix than for the iodine in the krypton matrix. By this, the principal effects found in iodine/krypton could be probably better resolved for the system chlorine/argon, since the contributions of different types of caging atoms could be more distinctive in the latter system. Another experimental motivation for this system is provided by the vibronic spectrum of chlorine in argon, which shows a nice separation of the zero phonon lines, which indicate the vibrational levels of the molecule, and the phonon side bands, which arise from interaction with the host atoms [20]. From Fig. 3.3, the $B(^3\Pi_u) \leftarrow X$ excitation spectrum of molecular chlorine in argon at 4 K, it can be seen that the phonon-side-bands will increase with the vibrational level excited.

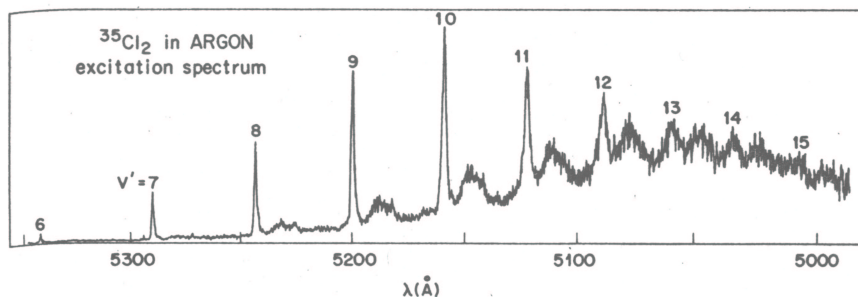


Figure 3.3: Excitation spectrum of $^{35}\text{Cl}_2$ in Ar with a ratio $\text{Cl}_2:\text{Ar}$ 1:3000, temperature 4 K. Taken from [20]

For the vibrational low levels, which belong to the bound part of the B-state, the interaction with the lattice atoms is much reduced, while the higher vibrational states are much more coupled to the lattice modes. Thus, the spectrum indicates a separable guest-host coupling, depending on the vibrational state of the guest molecule. This is apparent from the ratio of the intensity of zero phonon line and phonon side band, a large zero phonon line accompanied by a small phonon side band indicates a very small coupling for the vibrational states < 8 of the B-state. The system chlorine in argon is also subject of investigation of the group of Prof. Schwentner. Fig. 3.4 shows the pump-probe spectrum of Cl_2 in Ar to the $^1\Pi$ -states and to the $^3\Pi_0$ state.

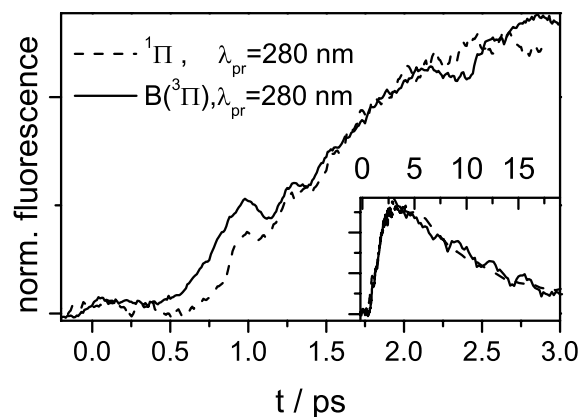


Figure 3.4: Pump-probe spectrum of Cl_2 in Ar. $\lambda_{\text{pump}} = 387 \text{ nm}$ ($^3\Pi_0$ excitation) and 290 nm ($^1\Pi_1$ excitation) [40]

The dynamics after excitation to the $^1\Pi$ state is nearly identical to that after excitation to the lower lying $^3\Pi$ state (see also Fig. 3.1). This indicates a state transition from the singlet to the triplet state, which was confirmed by the emission spectra of Cl_2 in Ar and could be initialized by interaction with the matrix. This spin flip was also observed for ClF in Ar and will be discussed in section 7.6. All spectra resulting from UV excitation can be connected to emission following excitation of the $^3\Pi$ state [71].

Excitation directly to the B-state of Cl_2 was also investigated in the group of Schwentner [40]. The pump-probe spectra show a complicated structure, see Fig. 3.5.

The spectra provide information about the oscillation periods and the anharmonicity of the potential and enables the determination of the rate for vibrational relaxation as discussed in section 1.5.1.1. The energy relaxation rate $k_{\text{rel}} = dE/dt$ as a function of excess energy shows an exponential behaviour, see Fig. 1.14, the same could be found for iodine in krypton [66]. At negative excess energies E_{excess} , the wavepacket will be in the bound part of the potential. By pumping high above the dissociation limit, at which E_{excess} will be 0, there will be a pronounced interaction with the cage, due to the high initial kinetic energy of the fragments, which would lead to dissociation in the gas phase, but is now repressed by the caging atoms. This means a collision will occur, in which a large amount of energy/momentum is transferred to the environment.

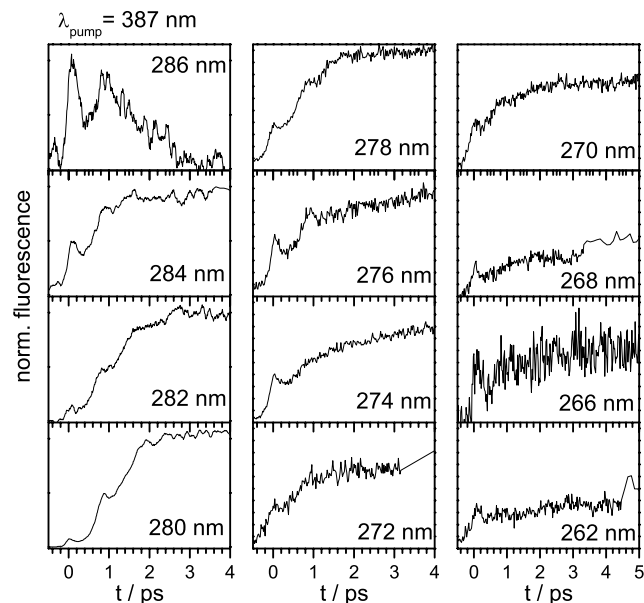


Figure 3.5: *Pump-probe spectrum of Cl_2 in Ar. $\lambda_{\text{pump}} = 387 \text{ nm}$ ($^3\Pi_0$ excitation) and different probe wavelength. Taken from M. Bargheer, Thesis [40]*

The decrease of the relaxation rate in the bound part of the potential will be much smoother, depending on the coupling strength to the environment and from Fig. 3.3 the coupling strength between chromophore and environment is expected to decrease in the course of vibrational relaxation. A detailed discussion will follow in section 6.7.1.6.

Another system, which was investigated thoroughly by theory is F_2 in Argon, as performed in the group of R.B. Gerber [22, 23, 42] by M. Niv, who gives a detailed overview of the system and the simulation method adopted in this work in her Ph.D. Thesis [42]. For F_2 in argon as the lightest dihalogen, quantum effects are not negligible and the semiclassical calculations were confirmed by exact quantum calculations based on the same DIM potentials including the two most important degrees of freedom [23]. A comparison will be given in section 7.7, see Fig. 7.16. Experimental data is not available.

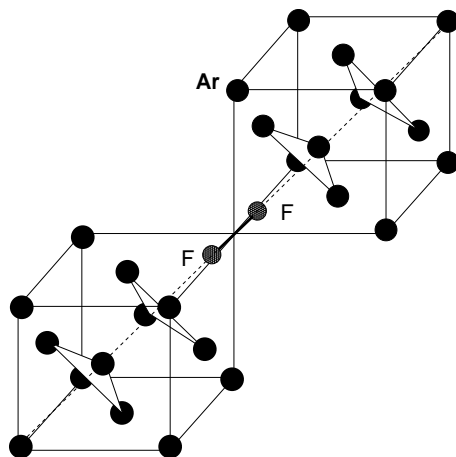


Figure 3.6: Orientation of F_2 in Ar: The molecule is aligned symmetric on the $\{111\}$ axis, pointing to triangular windows on each side.

F_2 in Ar occupies a single substitutional site in the lattice and is oriented in the $\{111\}$ direction as shown in Fig.3.6.

From this orientation we expect a different mechanism of the caging, as discussed in section 1.2. As was shown by semiclassical or quantum simulations, photoexcitation and subsequently dissociation of the fluorine molecule leads to collision of the atomic fragments with the windows. The momentum transfer connected to this collision event leads to an excitation of the Ar_3 stretching mode. This causes the windows to open and allows the cage exit of the fluorine fragments into the neighbouring cage, which is again restricted by a triatomic window, see Fig. 3.6. Pre-excitation of the Ar_3 stretching mode leads to an enhanced probability for the cage exit or dissociation of the chromophore. The system thus shows *delayed* cage exit, since the host atoms are not reoriented like in the mechanism of *forced* exit.

ClF in Ar, oriented in the same direction as F_2 in the $\{111\}$ direction could reveal insight in this mechanism of delayed exit as a different form of guest-host interaction. It has the advantage that experimental data is available [40, 78]. In addition, a different behaviour of the ClF atomic fragments could be expected, due to the different van-der-Waals radii and X-Rg potentials of fluorine or chlorine, respectively. Thus, the system should be suitable for investigations concerning the caging permitting comparison to experimental data.

In addition to the different mechanism of caging, pump-probe experiments showed another interesting effect: The molecule obviously undergoes an ultrafast state transition from the initially excited singlet Π to the 'forbidden' triplet Π state. The spectrum is shown in Fig. 3.7.

Fig. 3.7 shows the fluorescence at $\lambda_{LIF} = 420$ nm from one of the ionic states versus time delay t between the pump and probe pulse, as discussed in section 1.5. The arrows in panel a) indicate the motion of the wave packet, which is moving outward at 50 fs, and then inward after 500 fs. Excitation to the $^1\Pi$ state results in an increasing intensity after 2 ps after probing the $^3\Pi$ state, indicating a state transition to this triplet state. For longer times the spectrum for excitation to the singlet state fits the spectra for excitation to the triplet state, indicating complete state transition. Theoretical investigations have to be performed to reveal this mechanism of this ultrafast spin-flip.

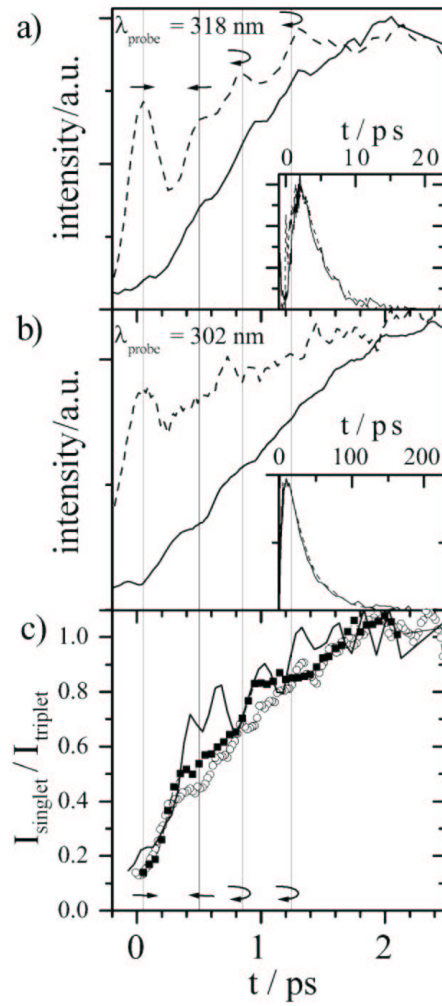


Figure 3.7: Pump-probe spectrum of ClF in Ar from probing the bound $^3\Pi$ states. a) dashed line: $\lambda_{\text{probe}} = 318 \text{ nm}$, excitation to $B^3\Pi_0$ with $\lambda_{\text{pump}} = 387 \text{ nm}$, solid line, excitation to $^1\Pi_1$ with $\lambda_{\text{pump}} = 280 \text{ nm}$; b) dashed line: $\lambda_{\text{probe}} = 302 \text{ nm}$, excitation to $B^3\Pi_0$ with $\lambda_{\text{pump}} = 387 \text{ nm}$, solid line: excitation to $^1\Pi_1$ with $\lambda_{\text{pump}} = 290 \text{ nm}$; c) ratio of $I_{\text{singlet}}/I_{\text{triplet}}$ for $\lambda_{\text{probe}} = 318 \text{ nm}$ with parallel polarization of pump and probe. The solid line is taken from [78], with relative polarization of pump and probe pulse. The arrows indicate the motion of the wave packet toward larger (\rightarrow) or smaller (\leftarrow) bond length and the probe pulse at the outer turning point (returning arrow). The small inserts of a) and b) show the spectra on a longer time scale. [78]